ARTICLE

Tanshinone IIA prevents LPS-induced inflammatory responses in mice via inactivation of succinate dehydrogenase in macrophages

Qiu-yan Liu[1], Yu Zhuang[1], Xian-rui Song[1], Qun Niu[1], Qiu-shuang Sun[1], Xiao-nan Li[2], Ning Li[3], Bao-lin Liu[1], Fang Huang[1] and Zhi-xia Qiu[4]

Metabolic reprogramming is associated with NLRP3 inflammasome activation in activated macrophages, contributing to inflammatory responses. Tanshinone IIA (Tan-IIA) is a major constituent from *Salvia miltiorrhiza* Bunge, which exhibits anti-inflammatory activity. In this study, we investigated the effects of Tan-IIA on inflammation in macrophages in focus on its regulation of metabolism and redox state. In lipopolysaccharides (LPS)-stimulated mouse bone marrow-derived macrophages (BMDMs), Tan-IIA (10 μM) significantly decreased succinate-boosted IL-1β and IL-6 production, accompanied by upregulation of IL-1RA and IL-10 release via inhibiting succinate dehydrogenase (SDH). Tan-IIA concentration dependently inhibited SDH activity with an estimated IC_{50} of 4.47 μM in LPS-activated BMDMs. Tan-IIA decreased succinate accumulation, suppressed mitochondrial reactive oxygen species production, thus preventing hypoxia-inducible factor-1α (HIF-1α) induction. Consequently, Tan-IIA reduced glycolysis and protected the activity of Sirtuin2 (Sirt2), an NAD^+-dependent protein deacetylase, by raising the ratio of NAD^+/NADH in activated macrophages. The acetylation of α-tubulin was required for the assembly of NLRP3 inflammasome; Tan-IIA increased the binding of Sirt2 to α-tubulin, and thus reduced the acetylation of α-tubulin, thus impairing this process. Sirt2 knockdown or application of Sirt2 inhibitor AGK-2 (10 μM) neutralized the effects of Tan-IIA, suggesting that Tan-IIA inactivated NLRP3 inflammasome in a manner dependent on Sirt2 regulation. The anti-inflammatory effects of Tan-IIA were observed in mice subjected to LPS challenge: pre-administration of Tan-IIA (20 mg/kg, ip) significantly attenuated LPS-induced acute inflammatory responses, characterized by elevated IL-1β but reduced IL-10 levels in serum. The peritoneal macrophages isolated from the mice displayed similar metabolic regulation. In conclusion, Tan-IIA reduces HIF-1α induction via SDH inactivation, and preserves Sirt2 activity via downregulation of glycolysis, contributing to suppression of NLRP3 inflammasome activation. This study provides a new insight into the anti-inflammatory action of Tan-IIA from the respect of metabolic and redox regulation.

Keywords: tanshinone IIA; lipopolysaccharides; succinate; SDH; HIF-1α; Sirt2; NLRP3 inflammasome; macrophages

INTRODUCTION

Macrophages are innate immune cells that shoulder the remarkable responsibility of rapidly responding to infections, injuries, or other pro-inflammatory stimuli, enhancing organism immunity and preventing organism damage [1, 2]. In response to infection or tissue damage, macrophages undergo metabolic reprogramming to enhance glycolysis in conditions of suppressed oxidative metabolism even under aerobic conditions. This phenotype is traditionally referred to as M1 activation [3, 4]. Accompanied by enhanced glycolysis, an increase in biosynthesis and an abnormal accumulation of metabolic intermediators are observed in activated macrophages, which is partially due to impaired oxidative metabolism in mitochondria [4–6]. Indeed, metabolic pauses are evident in the Krebs cycle, as indicated by citrate and succinate accumulation in M1 macrophages [7, 8]. In addition to

being a metabolic intermediator, many studies have increasingly demonstrated that succinate acts as an inflammatory signal to induce reactive oxygen species (ROS) generation in mitochondria and boost the inflammatory response [9, 10]. Succinate strongly induces IL-1β production through hypoxia-inducible factor-1α (HIF-1α) [11], since IL-1β is a direct target of HIF-1α. This indicates special roles for succinate and HIF-1α in the inflammatory response. In lipopolysaccharides (LPS)-stimulated macrophages, succinate directly inhibits the prolyl hydroxylase domain (PHD) to enhance the stability of HIF-1α because PHD induces HIF-1α degradation via hydroxylation of its proline residue [11, 12]. In addition, succinate also drives mitochondrial ROS production to indirectly increase HIF-1α stability rather than to impair PHD activity [8, 13]. As a transcription factor, HIF-1α enters the nucleus and transcriptionally upregulates target genes associated with

988

glycolysis and inflammatory cytokines to further support macrophage M1 activation. Therefore, the stabilization and accumulation of HIF-1α, which is jointly promoted by succinate accumulation and ROS generation, drive the polarization of macrophages and exacerbate the inflammatory response.

In activated macrophages, reprogrammed metabolism largely facilitates glycolysis, which inevitably reduces the NAD^+/NADH ratio by increasing the NADH content, leading to an imbalance in the cellular redox state [14]. Sirtuins (SIRTs) constitute a family of NAD^+-dependent protein deacetylases that are highly sensitive to energy status and the amount of NAD^+. Protein lysine acetylation is a key posttranslational modification in fuel metabolism, and SIRTs can influence protein function by the regulation of deacetylation [15]. Therefore, both NAD and SIRTs are emerging as pivotal regulators of inflammation. Enhanced glycolysis promotes the switch to NADH production, which can impair SIRT functions owing to their dependence on NAD^+ levels [16, 17]. SIRTs have consistently been proposed to defend against elevated ROS [18]. Among these subtypes of SIRTs (Sirt1–Sirt7), Sirtuin2 (Sirt2) is predominantly localized in the cytoplasm and colocalizes with microtubules, where it mediates the intracellular transport of organelles [19]. The microtubule network is constructed through the polymerization of acetylated α-tubulin, and Sirt2 determines the level of α-tubulin acetylation [20]. Microtubules are required for activation of the entire NLRP3 inflammasome [21]. A recent study reported the potential beneficial role of Sirt2 in suppressing NLRP3 activation by reducing the accumulation and polymerization of acetylated α-tubulin. Indeed, when the transcription or function of Sirt2 is inhibited, there would be an increase in acetylated α-tubulin that would promote the association of apoptosis-associated microparticle protein (ASC) with NLRP3. By recruiting caspase-1, the assembled NLRP3 inflammasome promotes IL-1β maturation and secretion [21, 22]. Considering the involvement of altered metabolism and the redox state, Sirt2 has emerged as an important mediator linking HIF-1α induction and the NLRP3 inflammasome, contributing to the inflammatory response in activated macrophages.

As a major constituent from *Salvia miltiorrhiza* Bunge, tanshinone IIA (Tan-IIA) has been substantially studied for its multifaceted health protection, including its favorable anti-inflammatory, antifibrotic, and antioxidative activities. Tan-IIA has been clinically used in China for the treatment of cardiovascular diseases [23–25]. Some researchers have reported that Tan-IIA exhibits anti-inflammatory benefits in regulating the release or expression of pro-inflammatory cytokines, such as IL-1β, IL-6, and TNF-α, in LPS-stimulated RAW 264.7 cells [26, 27]. Although many studies have demonstrated that Tan-IIA suppresses oxidative stress and inflammation [28, 29], this study predominantly investigated the effect of Tan-IIA on inflammation in macrophages from the perspective of metabolism and redox state regulation. In LPS-stimulated macrophages, Tan-IIA inactivated succinate dehydrogenase (SDH) and reduced HIF-1α induction via suppression of mitochondrial ROS production. As a consequence, Tan-IIA reduced α-tubulin acetylation by preserving Sirt2 induction, resulting in the prevention of NLRP3 inflammasome activation.

MATERIALS AND METHODS
Reagents
Tan-IIA (purity > 98%) was purchased from Aladdin (Shanghai, China). LPS, dimethyl succinate (DS, succinate analog), dimethyl malonate (DMM), oligomycin, rotenone, and tetramethylrhodamine ethyl ester perchlorate (TMRE) were all supplied by Sigma-Aldrich (St. Louis, MO, USA). The mitochondrial ROS scavenger mitTEMPO (mitT) and mitochondrial succinate transporter inhibitor diethyl butyl malonate (DEBM) were purchased from Sigma-Aldrich (St. Louis, MO, USA). The HIF-1α inhibitor PX-478 was supplied by Apexbio (APExBIO Technology LLC, Houston, USA). AGK-2 was provided by Dalian Meilun Biotechnology Co., LTD

(Dalian, China). These reagents were prepared in dimethylsulfoxide (DMSO) at the designated concentration and then were freshly diluted to the target concentration (the final concentration of DMSO was restricted to 0.1%, v/v).

Animals
Six-week-old male C57BL/6J mice (18–22 g) were purchased from SIPPR/BK Experimental Animal Co., Ltd. (Shanghai, China) and were allowed free access to water and food for a 1-week acclimation period that included 12 h light-dark cycles. The experiments were carried out in accordance with the recommendations of the Guide for the Care and Use of Laboratory Animals, and all animal experiments complied with the ARRIVE guidelines. The protocol (Approval No. 20190066) was approved by the Animal Care and Use Committee of China Pharmaceutical University (Nanjing, China).

For the LPS-challenged groups, mice were first intraperitoneally administered Tan-IIA (20 mg·kg^{-1}) or DMM (160 mg·kg^{-1}) 3 h before intraperitoneal injection with LPS (15 mg·kg^{-1}). After 2 h, blood was collected by tail bleeding to assess IL-1β and IL-10 levels with ELISA kits (IL-1β, CK-E20533M; IL-10, CK-E20005; Biocalvin, Suzhou, China). Mice were sacrificed by cervical dislocation, a small incision was made in the upper abdomen, and peritoneal macrophages were isolated and washed with 5 mL of ice-cold RPMI-1640 medium (containing 5% FBS). The cell suspension was pelleted in a cooled centrifuge for 10 min at $400 \times g$, and the collected macrophages were incubated for 24 h. Then, the levels of IL-1β, IL-10, and ROS were measured using commercial kits (IL-1β, CK-E20533M; IL-10, CK-E20005; Biocalvin, Suzhou, China; ROS, S0033, Beyotime Biotechnology, Shanghai, China). Moreover, the spleens were collected and homogenized to harvest protein for Western blot analysis.

Isolation and culture of bone marrow-derived macrophages (BMDMs) from mice
The preparation of BMDMs was performed as described in a previous work [30]. In brief, mice were sacrificed by cervical dislocation prior to the harvest of their femurs and tibia. The marrow was flushed out with cold RPMI-1640 (HyClone, USA). Afterwards, the supernatant was discarded, and an aliquot of red blood cell lysis buffer was added into the bottom layer to disaggregate the red cell pellet after pipetting up and down several times. The culture medium was replaced every other day with freshly prepared RPMI-1640 medium supplemented with 10% FBS and 20% L929 cell (depicted in the Supplementary information) supernatants. On day 6, the BMDMs were harvested after incubating them with PBS containing 10 mM EDTA, which was followed by vigorous pipetting several times. Eventually, the BMDM suspensions were cultured in RPMI-1640 medium supplemented with 10% FBS and 20% L929 cell supernatants for further experiments.

Macrophage polarization to the M1 phenotype in BMDMs and RAW 264.7 cells
After stimulation with LPS (100 ng·mL^{-1}) for 24 h, the gene expression levels of IL-1β, IL-12, arginase-1 (Arg-1), and IL-10 in BMDMs were analyzed by quantitative real-time PCR. Meanwhile, dimethyl succinate (DS, 5 mM) was supplemented with LPS (100 ng·mL^{-1}) to investigate the potential role of succinate in macrophage polarization. The levels of IL-1β, IL-6, IL-1RA, and IL-10 in BMDMs or RAW 264.7 cells (depicted in the Supplementary information) were determined by commercial ELISA kits (IL-1β, CK-E20533M; IL-10, CK-E20005; IL-6, CK-E20012; and IL-1RA, CK-E20121; Biocalvin, Suzhou, China).

Assays of succinate content, succinate dehydrogenase (SDH) activity, the NAD^+/NADH ratio, and lactate levels in BMDMs
After incubation with LPS (100 ng·mL^{-1}) for 24 h, assays were performed to measure the intracellular succinate content (JL46001, Jianglai Biotechnology, Shanghai, China), the ratio of

Tan-IIA alleviates inflammation via inactivation of SDH
QY Liu et al.

989

NAD$^+$/NADH (A019, Jiancheng Bioengineering Institute, Nanjing, China), and the SDH activity (A022, Jiancheng Bioengineering Institute, Nanjing, China) in cultured BMDMs or RAW 264.7 cells as well as the lactate released in the media (A019–2, Jiancheng Bioengineering Institute, Nanjing, China).

Detection of reactive oxygen species (ROS) generation in BMDMs
For the determination of intracellular ROS levels, BMDMs were pretreated with the indicated agents following LPS (100 ng ·mL^{-1}) or dimethyl succinate (DS, 5 mM) challenge. After 30 min, the cells were loaded with DCFH-DA (ROS-specific fluorescent probe, 10 µM; S003-1, Beyotime Biotechnology, Shanghai, China). Afterwards, the fluorescent intensity of the probe was measured by a microplate reader (Thermo Scientific, USA).

For mitochondrial ROS detection, BMDMs stimulated with LPS (100 ng· mL^{-1}) or DS (5 mM) for 24 h were separately loaded with the mitochondrial ROS-specific fluorescent probe MitoSOX Red (5 µM; M36008, Thermo Fisher Scientific, MA, USA), and then the cells were incubated for 30 min at 37 °C. After washing with PBS, the BMDMs were further incubated with MitoTracker (250 nM; 40742ES50, YEASEN Biotech, Shanghai, China) for another 30 min at 37 °C. For DS stimulation, BMDMs were simultaneously treated with oligomycin (ATP inhibitor) or rotenone (complex I inhibitor). After washing with PBS, the stained BMDMs were observed using laser confocal microscopy (LSM700, Zeiss, Germany).

As an assay of mitochondrial membrane potential detection, cells were incubated with LPS (100 ng ·mL^{-1}) or dimethyl succinate (DS, 5 mM) for 24 h, and then the medium was replaced with newly prepared RPMI-1640 medium supplemented with TMRE (500 nM; 87917, Sigma-Aldrich, MO, USA), and the cells were further incubated for another 20 min. Afterwards, TMRE staining was examined by inverted fluorescence microscopy (Olympus, Japan) or laser confocal microscopy (LSM700, Zeiss, Germany).

Immunofluorescence analysis of HIF-1α, NLRP3 inflammasome, ASC, and mitochondrial localization with endoplasmic reticulum
After the indicated treatments, BMDMs were fixed in 4% paraformaldehyde. Sequentially, 0.1% Triton and 5% BSA prepared in PBS were added to the cells and incubated for a specific time to block nonspecific staining. Immunofluorescent primary antibodies were added and incubated with the cells overnight at 4 °C. Additionally, the specific mitochondrial probe MitoTracker and the endoplasmic reticulum probe for the protein calreticulin (Anti-Calreticulin, ab92516, Abcam, Cambridge, UK) were added separately to assess the localization of the mitochondria and endoplasmic reticulum. After washing the cells, the immunofluorescence analysis of specific proteins was viewed by laser confocal microscopy (LSM700, Zeiss, Germany).

Small interfering RNA transfection
To investigate the function of Sirt2 in the acetylation of α-tubulin, BMDMs were transfected with a small interfering RNA targeting Sirt2 or with a control siRNA (GenePharma, Suzhou, China) to silence Sirt2. Lipofectamine 2000 reagent (Invitrogen, CA, USA) was employed to transfect BMDMs cells. After 24 h of transfection, the cells were cultured in freshly prepared RPMI-1640 medium for subsequent experiments (replacement with fresh RPMI-1640 medium was aimed at minimizing possible cell damage and ruling out possible interference caused by the transfection reagent).

Western blot and immunoprecipitation analysis
BMDM lysates were prepared by lysing the cells for 45 min using RIPA buffer (containing PMSF) in an ice bath. Similarly, RIPA lysate (including PMSF) was added to spleen slices (~30 mg) in an ice bath, and then they were ground with a glass homogenizer. Then, the homogenates of the BMDMs or spleens were centrifuged at 12,000 rpm for 15 min at 4 °C, and the supernatants were collected. The protein concentrations were quantified by commercial BCA kits (Jiancheng Bioengineering Institute, Nanjing, China). Equal amounts of proteins were loaded and separated by SDS-PAGE and then were transferred to PVDF membranes, which was followed by blocking at ambient temperature for 2 h. Subsequently, the following specific primary antibodies were incubated with the membranes overnight at 4 °C: anti-HIF-1α (#36169, Cell Signaling Technology Inc., MA, USA), anti-IL-1β (#12242, Cell Signaling Technology Inc., MA, USA), anti-NLRP3 (AG-20B-0014-C100, Adipogen, CA, USA), anti-caspase-1 (ab207802, Abcam, Cambridge, UK), anti-acetylated-α-tubulin (acetyl K40) antibody (ab179484, Abcam, Cambridge, UK), and anti-acetylated-lysine (#9441, Cell Signaling Technology Inc., MA, USA). Then, the corresponding secondary antibodies (goat anti-rabbit, SA00001-2, Proteintech, IL, USA) were incubated with the membranes. GAPDH (AP0063, Bioworld Technology Inc., MN, USA) was used as a reference protein. The development was performed with ECL-enhanced chemiluminescence (Yeasen, Shanghai, China) and was quantified by ImageJ software (National Institutes of Health).

For immunoprecipitation, the supernatants of lysates were harvested after centrifugation at 12,000 rpm for 15 min. Anti-rabbit IgG (H + L)-FITC (BS10950), goat anti-rabbit IgG (H + L) HRP (BS13278), and goat anti-mouse IgG (H + L) HRP (BS12478) were all purchased from Bioworld Technology (MN, USA). Anti-α-tubulin (11224-1-AP, Proteintech, IL, USA), anti-NLRP3, anti-ASC (#67824, Cell Signaling Technology Inc., MA, USA), anti-Sirt1 (#9475, Cell Signaling Technology Inc., MA, USA), and anti-Sirt2 (AP0019, Bioworld Technology Inc., MN, USA) antibodies were incubated with the supernatants separately overnight at 4 °C and then were immunoprecipitated with protein A + G agarose beads (SC2003, Santa Cruz Biotechnology, CA, USA) for another 2 h according to the protocols. Then, Western blotting was performed with the indicated antibodies.

Quantitative real-time PCR
Total RNA was extracted from BMDMs with TRIzol reagent (KeyGEN Bio TECH, China), and the concentration and purity of the RNA were determined using an ultramicro spectrophotometer (Nano-100, Hangzhou Allsheng Instruments Co., Ltd. Hangzhou, China). Next, the RNA was reverse transcribed to generate cDNA using All-In One-RT Master Mix synthesis kits (Applied Biological Materials Inc., Canada). Real-time PCRs were performed using a Hieff^{TM} qPCR SYBR Green Master Mix Kit (Yeasen, Shanghai, China) with primers for IL-1β, IL-12p40, Arg-1, IL-10, pyruvate kinase M2 isoform (PKM2), hexokinase 2 (HK-II), and β-actin (summarized in Table S1 in the Supplementary information) and a CFX96^{TM} real-time system (BIO-RAD, USA). The mRNA levels of target genes were normalized to β-actin levels and were compared by the $2^{-\Delta\Delta Ct}$ method.

Statistical analysis
Experimental data are expressed as the mean ± SD of at least three independent experiments (the final sample number is depicted in the legend below each figure). Statistical analysis was performed using GraphPad Prism 7.0 (San Diego, CA, USA) by applying one-way ANOVA (comparing among more than two groups) or two-tailed Student's t tests (comparison between two groups), and $P < 0.05$ was considered statistically significant.

RESULTS
Tan-IIA regulated macrophage polarization with SDH inhibition in BMDMs
In the process of immunoregulation, macrophages exhibit high plasticity, which is characterized by M1 and M2 polarization [5, 31].

Tan-IIA alleviates inflammation via inactivation of SDH
QY Liu et al.

990
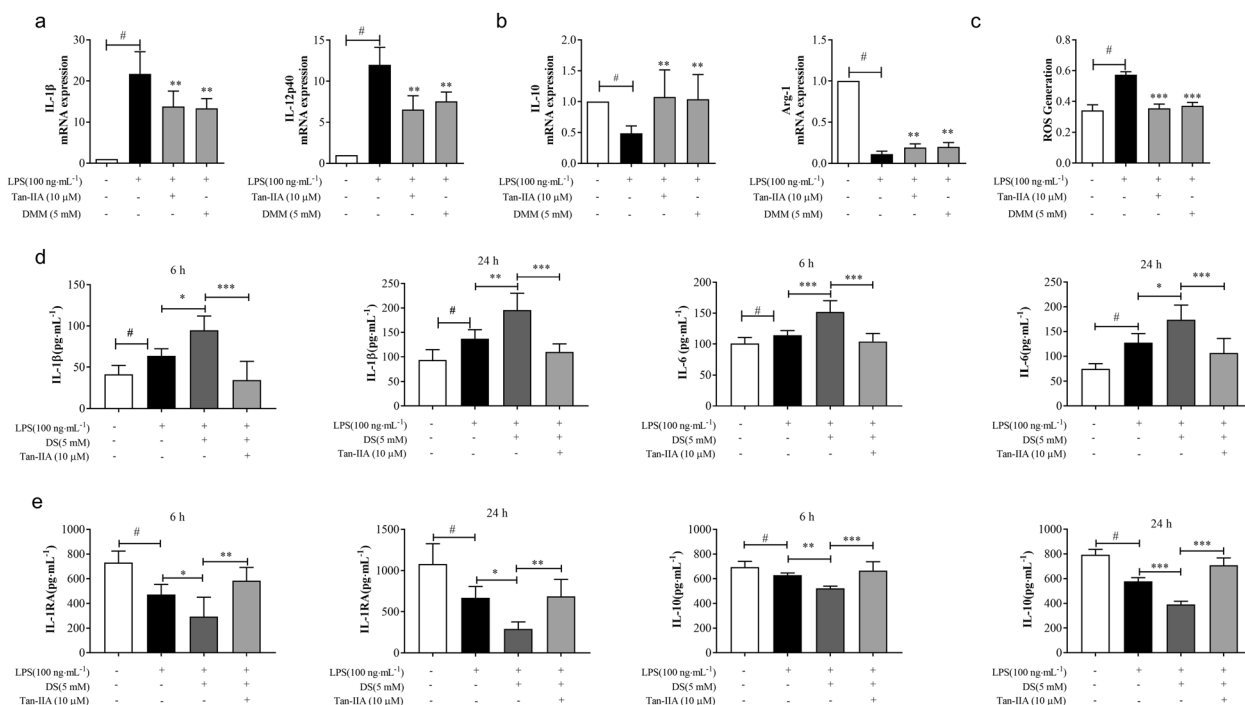
Fig. 1 Tan-IIA attenuated the inflammatory response in macrophages. a, **b** The gene expression of IL-1β, IL-12, IL-10, and Arg-1 in BMDMs stimulated with LPS (100 ng·mL^{-1}) for 24 h; **c** intracellular ROS production in BMDMs stimulated with LPS (100 ng·mL^{-1}) for 24 h; **d**, **e** protein production of IL-1β, IL-6, IL-1RA, and IL-10 in the supernatants of BMDMs exposed to LPS (100 ng·mL^{-1}) plus DS (5 mM) for 6 or 24 h (Tan-IIA tanshinone IIA, DMM dimethyl malonate, DS dimethyl succinate). Data are expressed as the mean ± SD, $n = 5$; *$P < 0.05$, **$P < 0.01$, ***$P < 0.001$ vs. LPS-stimulated BMDMs; #$P < 0.05$ vs. blank.

An LPS challenge significantly induced the gene expression of IL-1β and IL-12p40 in BMDMs compared to that of controls (Fig. 1a). In contrast, the gene expression of the anti-inflammatory cytokines IL-10 and Arg-1 was reduced (Fig. 1b). Tan-IIA (10 μM) significantly reversed these gene expression alternations, demonstrating its ability to prevent the macrophage polarization switch toward the M1 phenotype. Moreover, the increased generation of intracellular ROS was restricted by Tan-IIA (Fig. 1c). Similar regulation was also observed in RAW 264.7 cells stimulated by LPS (Fig. S1 in the Supplementary information). Similar to Tan-IIA, the SDH inhibitor DMM suppressed the inflammatory response in LPS-stimulated macrophages (Fig. 1a–c), suggesting the involvement of SDH in macrophage activation. In LPS-activated BMDMs, cell permeable diethyl succinate (DS, 5 mM) was used to increase the intracellular succinate levels. DS significantly increased the release of IL-1β and IL-6 but decreased the production of IL-1RA and IL-10, as measured in the supernatants of BMDM cultures harvested at different times (Fig. 1d, e). Tan-IIA effectively inhibited succinate-mediated increases in IL-1β and IL-6 production, which was accompanied by upregulated release of IL-1RA and IL-10 (Fig. 1d, e); these findings raise the possibility that Tan-IIA inhibited macrophage polarization to the M1 phenotype via SDH inactivation.

Tan-IIA inhibited SDH activity by suppressing mitochondrial ROS production

Next, we examined the effect of Tan-IIA on SDH activity in LPS-activated BMDMs and found that Tan-IIA inhibited SDH activity in a concentration-dependent manner, with an estimated IC$_{50}$ of 4.47 μM (Fig. 2a). Meanwhile, LPS-induced succinate accumulation was reduced by Tan-IIA (Fig. 2b). When DS (5 mM) was used as the substrate to activate SDH in macrophages, the increase in SDH activity was effectively inhibited by Tan-IIA (Fig. 2c). It has been reported that Tan-IIA can insert into the pocket of SDH through

hydrogen bonding with two amino acid residues, ALA71 and THR99, that surround the pocket [32].

Macrophage activation is closely associated with ROS production, while succinate oxidation by SDH extensively drives mitochondrial ROS production to activate the inflammatory response. Under laser confocal microscopy observation with the specific fluorescent probe MitoSOX/MitoTracker, we observed that succinate boosted mitochondrial ROS production in LPS-stimulated BMDMs, whereas the increased ROS production was suppressed by Tan-IIA and DMM (Fig. 2d). In activated macrophages, SDH activation-induced mitochondrial ROS production is a result of reverse electron transfer (RET), which occurs because of an increase in mitochondrial membrane potential (Δψ$_m$). To establish RET in macrophages, we inhibited ATP synthase with oligomycin (4 μM), while succinate was used as the substrate of SDH, and the increase in mitochondrial ROS production was reduced by Tan-IIA and DMM (Fig. 2e). The mitochondrial complex I inhibitor rotenone (1 μM) reduced mitochondrial ROS production, indicating that ROS are generated by mitochondrial complex I due to RET (Fig. 2f). Tan-IIA and DMM inhibited SDH activity and contributed to downregulating Δψ$_m$ in LPS-activated macrophages (Fig. 2f). In support of this conclusion, succinate-induced high Δψ$_m$ was reduced by Tan-IIA and DMM (Fig. 2g). Together, these data provide evidence that Tan-IIA suppresses mitochondrial ROS production via SDH inhibition in LPS-activated macrophages.

Tan-IIA attenuated HIF-1α induction and reduced glycolysis

HIF-1α is a transcription factor that regulates genes encoding proteins that promote glycolysis to support macrophage M1 activation [12]. HIF-1α is constantly synthesized and rapidly degraded by PHDs dioxygenases, while ROS can impair PHD to prevent HIF-1α degradation [11]. LPS challenge significantly promoted the protein expression of HIF-1α, whereas the induction

Tan-IIA alleviates inflammation via inactivation of SDH
QY Liu et al.

991
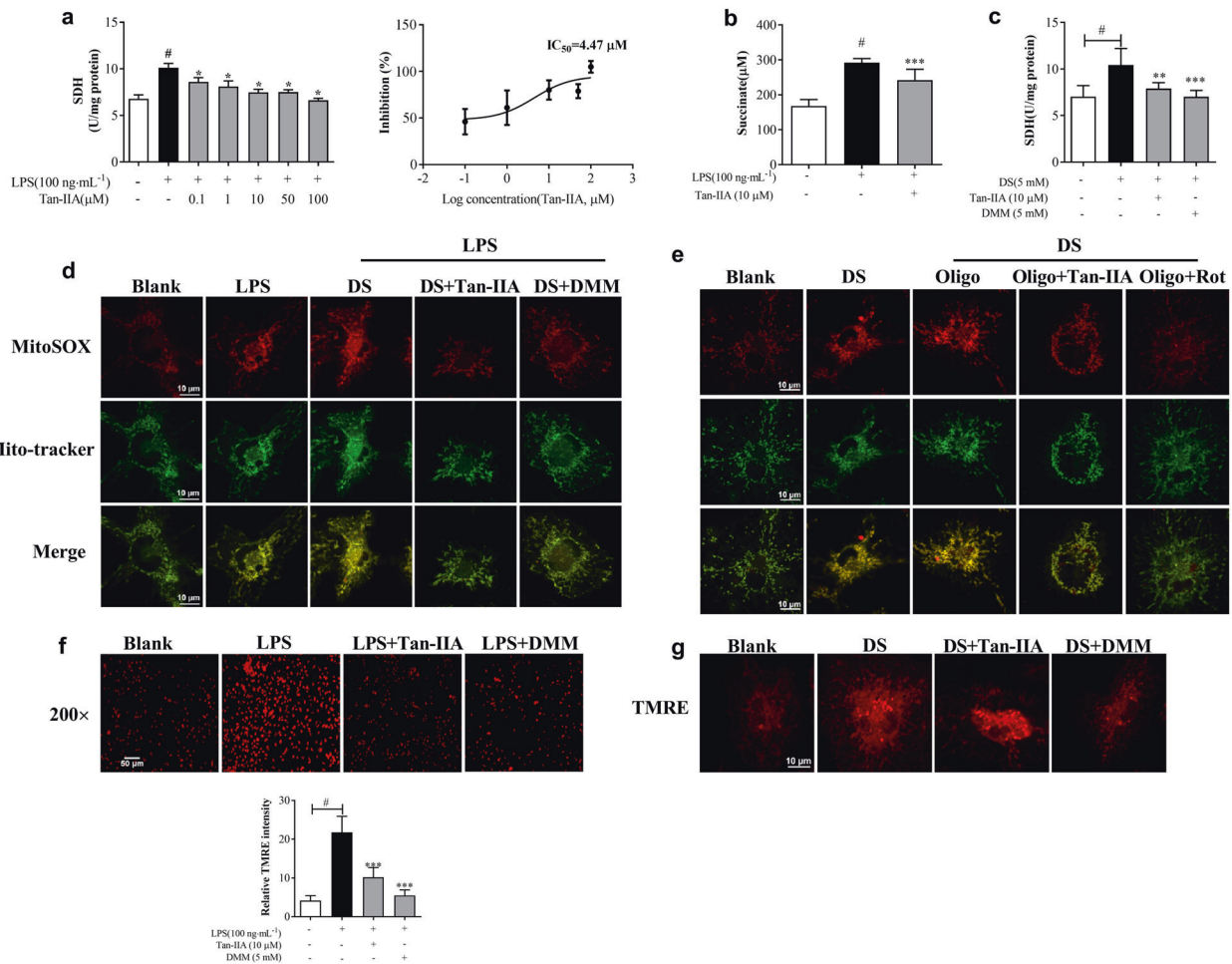
Fig. 2 Tan-IIA inhibited SDH activity by suppressing mitochondrial ROS production in BMDMs. a SDH activity in BMDMs stimulated with LPS (100 ng·mL^{-1}) for 24 h with Tan-IIA ranging from 0.1–100 μM; **b** succinate accumulation in BMDMs stimulated with LPS (100 ng·mL^{-1}) for 24 h; **c** SDH activity in BMDMs exposed to LPS (100 ng·mL^{-1}) plus DS (5 mM) for 24 h; **d** MitoSOX and MitoTracker fluorescent probe staining to measure ROS production in BMDMs exposed to LPS (100 ng·mL^{-1}) plus DS (5 mM) for 30 min (scale bar, 10 μm); **e** MitoSOX and MitoTracker fluorescent probe staining to indicate ROS production in BMDMs exposed to DS (5 mM) or DS plus Oligo (4 μM) or DS plus Oligo (4 μM) and Rot (1 μM) for 30 min (scale bar, 10 μm); **f, g** mitochondrial membrane potential in BMDMs stimulated with LPS (100 ng·mL^{-1}) or DS (5 mM) for 20 min, as observed by fluorescent inverted microscope (scale bar, 50 μm) or laser confocal microscopy (scale bar, 10 μm) (Tan-IIA tanshinone IIA, DMM dimethyl malonate, DS dimethyl succinate, Oligo oligomycin, Rot rotenone, TMRE tetramethylrhodamine ethyl ester). Data are expressed as the mean ± SD, $n = 5$; *$P < 0.05$, **$P < 0.01$, ***$P < 0.001$ vs. LPS-stimulated BMDMs; #$P < 0.05$ vs. blank.

was significantly attenuated by Tan-IIA and DMM (Fig. 3a). The mitochondrial ROS scavenger mitT countered LPS-stimulated HIF-1α induction (Fig. 3b), indicating that mitochondrial ROS was a driving force for HIF-1α induction. Moreover, the mitochondrial succinate transporter inhibitor DEBM also reduced the levels of HIF-1α protein, which partly demonstrated that elevated cytosolic succinate led to upregulated HIF-1α. As a consequence, succinate evidently promoted the nuclear translocation of HIF-1α, while Tan-IIA and DMM effectively blocked this transition in response to DS (Fig. 3c). In LPS-activated macrophages, the elevation in glycolysis was supported by the upregulated gene expression of HK-II and PKM2 (Fig. 3d), as well as the accumulated amount of lactate (Fig. 3e). However, Tan-IIA distinctly inhibited the expression of HK-II and PKM2 (Fig. 3d) and subsequently reduced lactate production (Fig. 3e). The HIF-1α inhibitor PX-478 attenuated HK-II and PKM2 gene expression, which was indicative of the involvement of HIF-1α in the expression of glycolysis-related genes (Fig. 3d). Tan-IIA increased the redox state in LPS-activated macrophages, as evidenced by the increased ratio of NAD$^+$/NADH (Fig. 3f); this increase is likely due to the preserved NAD$^+$ levels via the downregulation of glycolysis.

Tan-IIA reduced α-tubulin acetylation by Sirt2 induction

In LPS-activated macrophages, the accumulated succinate functions as an inflammatory signal to induce the secretion of IL-1β [11]. In fact, IL-1β maturation indispensably requires cysteine protease (caspase-1) to cleave the IL-1β precursor. The assembly of the NLRP3 inflammasome leads to caspase-1-dependent signaling [33]. Hence, the promotion of IL-1β secretion indicated that IL-1β maturation was probably mediated by NLRP3 inflammasome activation. Because α-tubulin acetylation is required for NLRP3 inflammasome assembly, we wondered whether Tan-IIA prevented NLRP3 inflammasome activation by regulating α-tubulin acetylation. SIRTs are a family of NAD$^+$-dependent protein deacetylases, and consistent with the reduction in NAD$^+$ levels, the gene expression of SIRTs, (Sirt1–3) was reduced in LPS-activated macrophages (Figs. 4a and S2, in the Supplementary information). Sirt3 is mainly located in mitochondria, while Sirt1 and Sirt2 are predominantly distributed in the cytosol. Because Sitr2 has been documented to mediate the deacetylation of α-tubulin in the cytosol, we examined the effects of Tan-IIA on Sirt2 induction. In addition to the effect on the gene expression of Sirt2, Tan-IIA promoted the level of Sirt2 protein in a concentration-

Tan-IIA alleviates inflammation via inactivation of SDH
QY Liu et al.

992
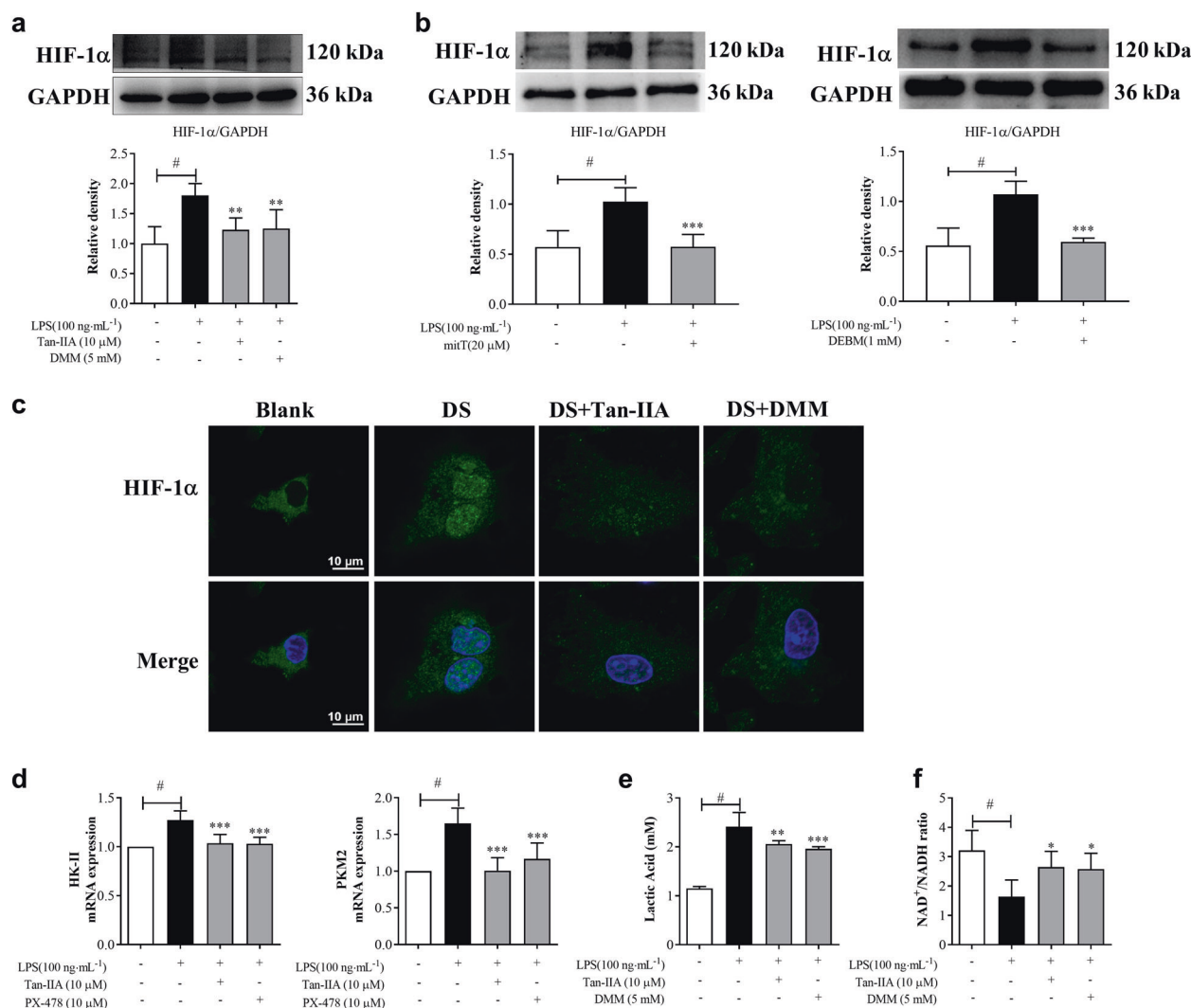
Fig. 3 Tan-IIA attenuated HIF-1α induction and reduced glycolysis in BMDMs. a, b HIF-1α expression in BMDMs stimulated with LPS (100 ng·mL^{-1}) in the presence of mitT (20 μM) or DEBM (1 mM) for 24 h; **c** the nuclear translocation of HIF-1α in BMDMs treated with DS (5 mM) for 24 h (scale bar, 10 μm); **d** the gene expression of HK-II and PKM2 in BMDMs stimulated with LPS (100 ng·mL^{-1}) for 24 h in the presence or absence of PX-478 (10 μM); **e** intracellular content of lactate in BMDMs stimulated with LPS (100 ng·mL^{-1}) for 24 h; **f** NAD$^+$/NADH ratio in BMDMs stimulated with LPS (100 ng·mL^{-1}) for 24 h (Tan-IIA tanshinone IIA, DMM dimethyl malonate, DS dimethyl succinate, mitT mitTEMPO, DEBM diethyl butyl malonate). Data are expressed as the mean ± SD, $n = 5$; *$P < 0.05$, **$P < 0.01$, ***$P < 0.001$ vs. LPS-stimulated BMDMs; #$P < 0.05$ vs. blank.

dependent manner (Fig. 4b). Further results also showed that Tan-IIA and DMM increased Sirt2 gene expression and attenuated the acetylation of cytosolic protein in LPS-activated macrophages (Fig. 4a, b). Moreover, the acetylation of α-tubulin was further confirmed by determining the ratio between acetylated α-tubulin and α-tubulin (Fig. 4c). The immunoprecipitation results showed that Sirt2, but not Sirt1, bound to α-tubulin (Fig. 4d). Tan-IIA increased the binding of Sirt2 to α-tubulin, which reduced the acetylation of α-tubulin (Fig. 4d, e). These results suggested that Tan-IIA reduced α-tubulin acetylation by preserving Sirt2 induction. Sirt2 gene silencing by siRNA transfection increased α-tubulin acetylation, and Tan-IIA failed to influence this increase (Fig. 4g, h), providing evidence to support this conclusion. In conclusion, Tan-IIA regulated the activity of Sirt2 by influencing its expression, other than affecting the level of NAD$^+$/NADH (Fig. 3f), since NAD$^+$ is indispensably required for Sirt2 function.
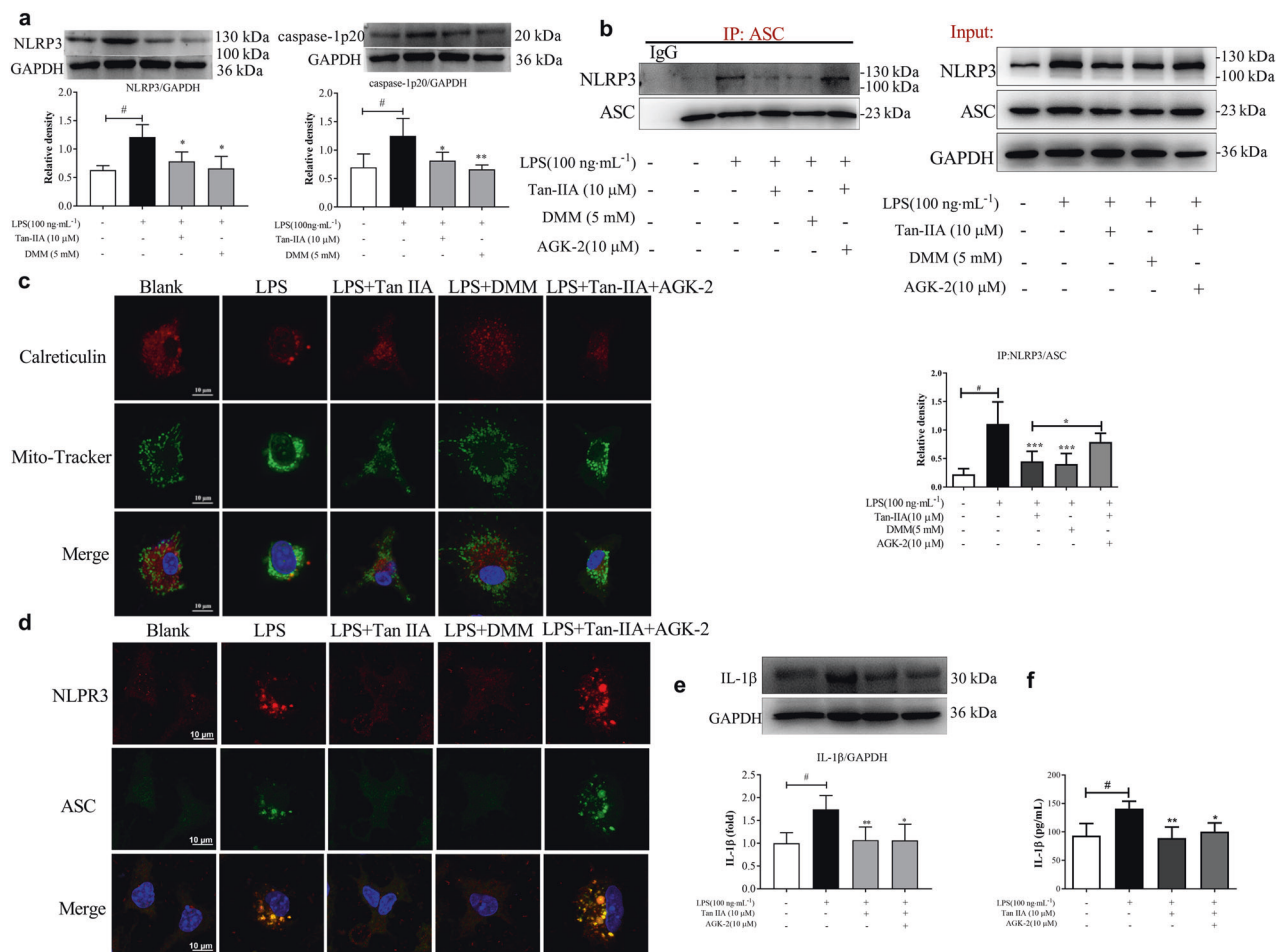
Tan-IIA inactivated the NLRP3 inflammasome by promoting Sirt2
As the most structurally and functionally complex inflammasomes, the NLRP3 inflammasome is assembled by NLRP3, apoptosis-

associated microparticle protein (ASC) and caspase-1 after the cell encounters inflammatory stimuli [21, 22]. LPS challenge profoundly upregulated the protein levels of both NLRP3 and caspase-1, which was reversed by either Tan-IIA or DMM treatment (Fig. 5a). The immunoprecipitation results showed that Tan-IIA and DMM blocked the interaction between NLRP3 and ASC. However, the Sirt2 inhibitor AGK-2 significantly offset the effects of Tan-IIA on the abovementioned interaction (Fig. 5b). Immunofluorescent staining using laser confocal microscopy demonstrated that the endoplasmic reticulum (stained by calreticulin) and mitochondria (stained by MitoTracker) drove the translocation of the two organelles to the perinuclear space for assembly, but the shift in localization was abrogated by Tan-IIA treatment (Fig. 5c). Next, we used anti-NLRP3 and anti-ASC antibodies to immunocytochemically determine their distribution to further verify the colocalization of NLRP3 and ASC, as shown in Fig. 5d. When the mitochondria approached the endoplasmic reticulum, the colocalization of ASC (located in the mitochondria) and NLRP3 (localized in the endoplasmic reticulum) promoted the assembly of the NLRP3 inflammasome, while Tan-IIA impaired

Tan-IIA alleviates inflammation via inactivation of SDH
QY Liu et al.

993
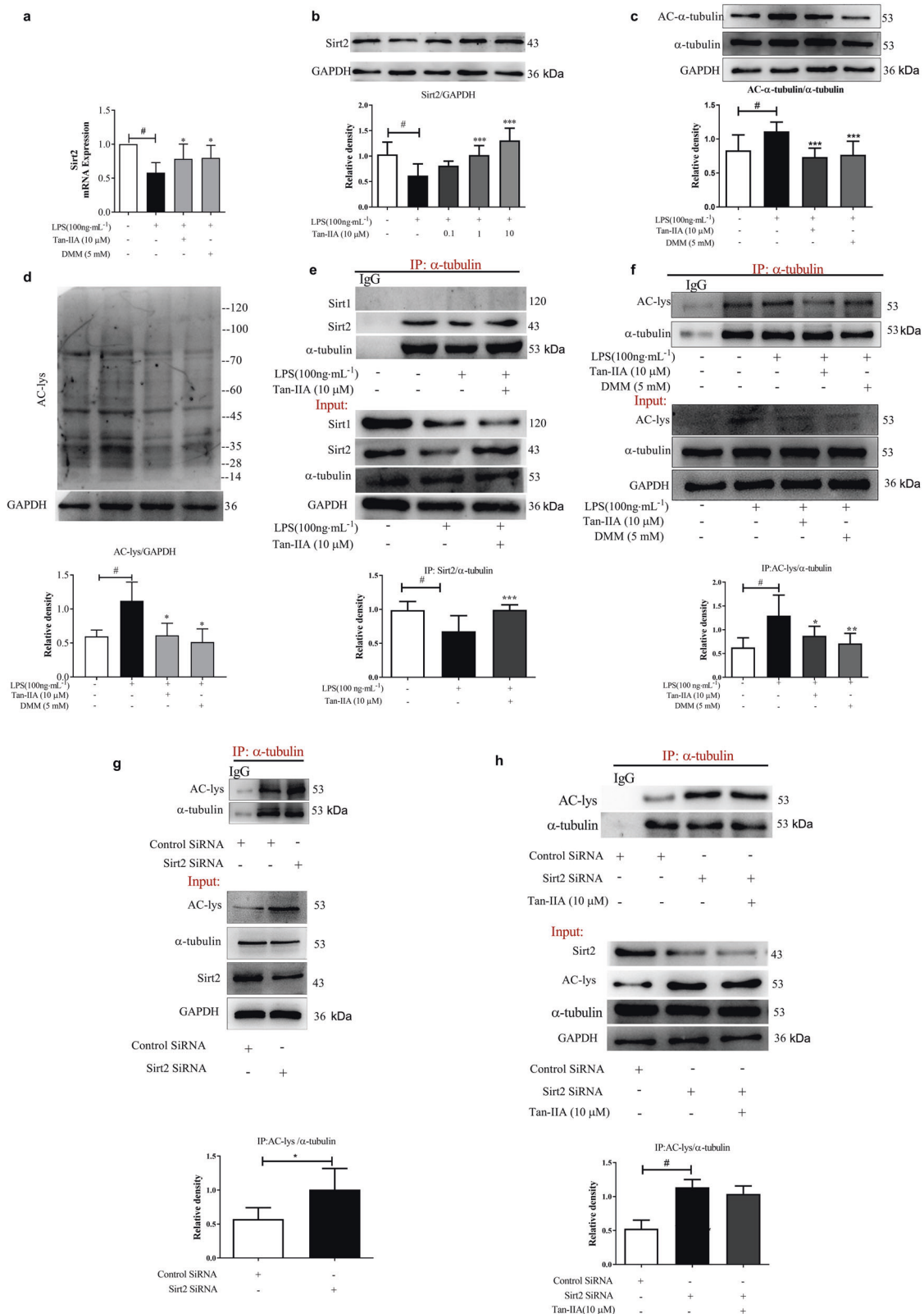
Fig. 4 Tan-IIA reduced α-tubulin acetylation by Sirt2 induction in BMMDs. a Gene expression of Sirt2 in BMDMs stimulated with LPS (100 ng· mL^{-1}) for 24 h; **b** protein expression of Sirt2 in LPS (100 ng· mL^{-1}) stimulated BMDMs for 24 h; **c** protein expression of acetylated α-tubulin in BMDMs stimulated with LPS (100 ng ·mL^{-1}) for 24 h; **d** intracellular protein acetylation in BMDMs stimulated with LPS (100 ng ·mL^{-1}) for 24 h; **e** immunoprecipitation analysis of the binding of Sirt1 or Sirt2 to α-tubulin in BMDMs stimulated with LPS (100 ng ·mL^{-1}) for 24 h; **f** immunoprecipitation analysis of α-tubulin acetylation in BMDMs stimulated with LPS (100 ng· mL^{-1}) for 24 h; **g, h** immunoprecipitation analysis of α-tubulin acetylation in BMDMs transfected with a small interfering RNA targeting Sirt2 for 24 h (Tan-IIA tanshinone IIA, DMM dimethyl malonate, Sirt2 Sirtuin2). Data are expressed as the mean ± SD, $n = 5$; *$P < 0.05$, **$P < 0.01$, ***$P < 0.001$ vs. LPS-stimulated BMDMs; #$P < 0.05$ vs. blank.

Tan-IIA alleviates inflammation via inactivation of SDH
QY Liu et al.

994

Fig. 5 Tan-IIA inactivated NLRP3 inflammasome activation through Sirt2 signaling in BMDMs. a The protein expression of NLRP3 and caspase-1 in BMDMs stimulated with LPS (100 ng · mL⁻¹) for 24 h; **b** immunoprecipitation analysis of the binding of NLRP3 to ASC in BMDMs stimulated with LPS (100 ng · mL⁻¹) for 24 h; **c** laser confocal images of the colocalization of mitochondria (stained by MitoTracker) and endoplasmic reticulum (stained by calreticulin) in BMDMs stimulated with LPS (100 ng · mL⁻¹) or LPS (100 ng · mL⁻¹) plus AGK-2 (10 µM) for 30 min (scale bar, 10 µm); **d** laser confocal images of NLRP3 and ASC transposition to the perinuclear space in BMDMs stimulated with LPS (100 ng · mL⁻¹) or LPS (100 ng · mL⁻¹) plus AGK-2 (10 µM) for 30 min (scale bar, 10 µm); **e** protein expression of IL-1β in BMDMs stimulated with LPS (100 ng · mL⁻¹) or LPS (100 ng · mL⁻¹) plus AGK-2 (10 µM) for 30 min; **f** IL-1β secretion from BMDMs stimulated with LPS (100 ng · mL⁻¹) in the presence or absence of AGK-2 (10 µM) for 24 h (Tan-IIA tanshinone IIA, DMM dimethyl malonate). Data are expressed as the mean ± SD, $n = 5$. *$P < 0.05$, **$P < 0.01$, ***$P < 0.001$ vs. LPS-stimulated BMDMs; #$P < 0.05$ vs. blank.

assembly by disrupting the shift in localization of the endoplasmic reticulum. As expected, Tan-IIA impaired the expression and maturation of IL-1β (Fig. 5e, f). The Sirt2 inhibitor AGK-2 diminished the inhibitory effects of Tan-IIA, suggesting that Sirt2 activation by Tan-IIA contributed to the prevention of NLRP3 inflammasome assembly.
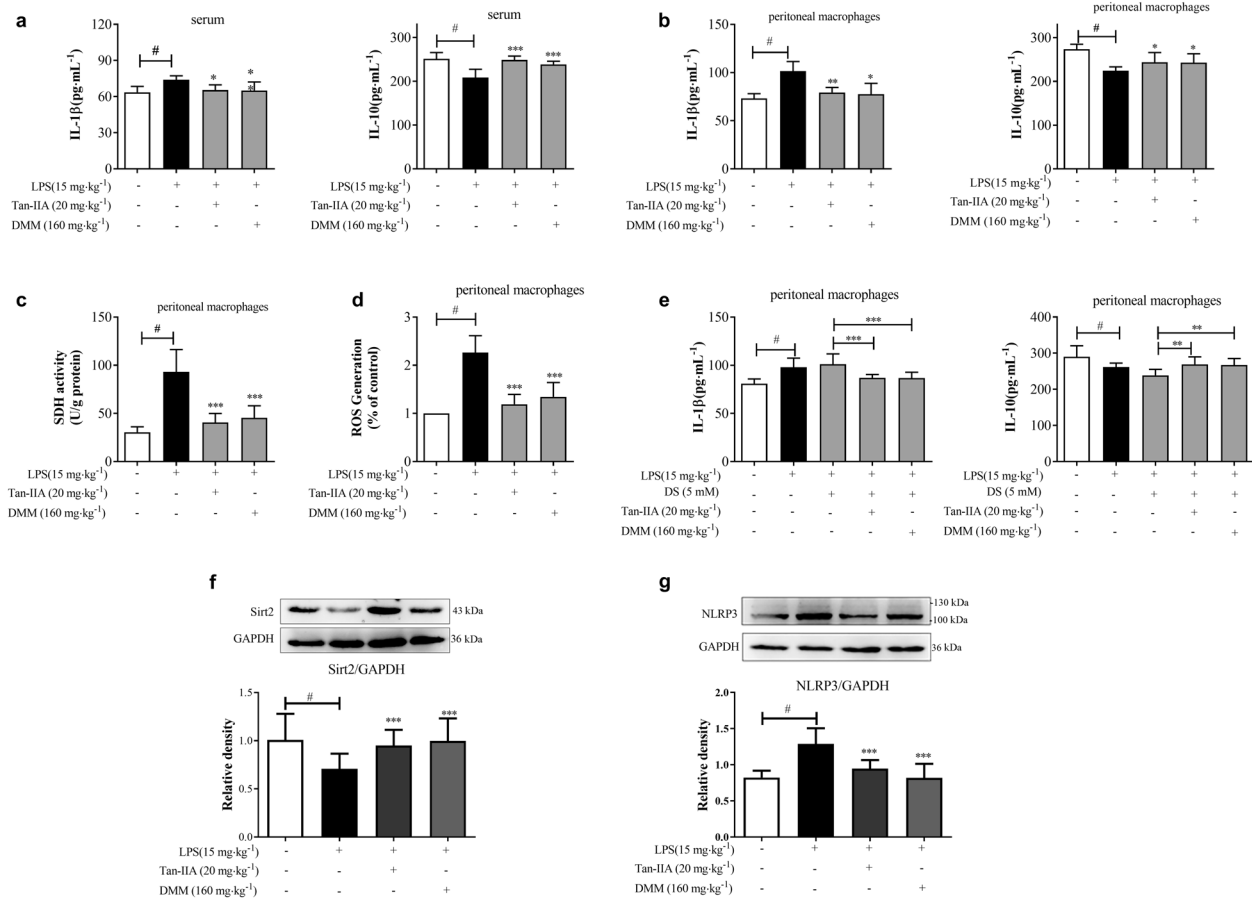
Tan-IIA suppressed the inflammatory response in vivo
Mice subjected to an LPS challenge exhibited an acute inflammatory response, characterized by elevated IL-1β and reduced IL-10 levels in serum; however, this response was attenuated by Tan-IIA and DMM administration (Fig. 6a). Similar regulation was also observed in peritoneal macrophages isolated from mice subjected to an LPS challenge (Fig. 6b). Consistently, Tan-IIA suppressed SDH activity with reduced ROS production in peritoneal macrophages (Fig. 6c, d). When exogenous succinate was supplemented to increase inflammation, reduced IL-1β release and increased IL-10 production were observed in peritoneal macrophages prepared from mice treated with Tan-IIA and DMM before LPS challenge (Fig. 6e). Tan-IIA promoted the expression of Sirt2 protein in mice stimulated by LPS; consequently, Tan-IIA reduced the expression of NLRP3 protein (Fig. 6f, g). These results confirmed that Tan-IIA

inhibited SDH activity and suppressed the inflammatory response in mice, which was partially due to the suppression of NLRP3 inflammasome activation via Sirt2 induction.

DISCUSSION
Many studies have confirmed that succinate, an intermediate in metabolism, functions in signal transduction in ROS generation and the inflammatory response [11, 34]. The upregulated mitochondrial oxidation of succinate via SDH drives ROS production [10]. When macrophages are stimulated by LPS, the core intracellular metabolism is transformed from mitochondrial oxidative phosphorylation to cytosolic glycolysis to satisfy the demands of energy [6, 35]. The alteration to mitochondrial respiration serves as a crucial regulator of the body's immune response [4, 35]. It has been reported that metabolic shifting increases succinate accumulation and SDH activity to boost the inflammatory response in activated macrophages [10]. Recent studies have indicated that LPS triggers the inflammatory response by promoting the activity of SDH [10, 11]. In the present study, we showed that succinate served as an inflammatory molecule that induced NLRP3 inflammasome activation via HIF-1α

Tan-IIA alleviates inflammation via inactivation of SDH
QY Liu et al.

995

Fig. 6 **Tan-IIA suppressed the inflammatory response in mice subjected to LPS challenge. a** The levels of IL-1β and IL-10 in the serum of mice subjected to LPS challenge (15 mg· kg^{-1}; after drug administration for 3 h, the samples were collected); **b** the intracellular levels of IL-1β and IL-10 in isolated peritoneal macrophages from mice subjected to LPS challenge (15 mg· kg^{-1}); **c, d** SDH activity and mitochondrial ROS production in isolated peritoneal macrophages from mice subjected to LPS challenge (15 mg· kg^{-1}); **e** the intracellular levels of IL-1β and IL-10 in isolated peritoneal macrophages from mice subjected to LPS challenge (15 mg· kg^{-1}) when exposed to endogenous succinate (DS, 5 mM) (Tan-IIA tanshinone IIA, DMM dimethyl malonate, DS dimethyl succinate); **f** protein expression of Sirt2 in the spleens of mice subjected to LPS challenge (15 mg· kg^{-1}); **g** protein expression of NLRP3 in spleen of mice subjected to LPS challenge (15 mg· kg^{-1}). Data are expressed as the mean ± SD, $n = 8$ in each group. *$P < 0.05$, **$P < 0.01$, ***$P < 0.001$ vs. LPS-challenged mice; #$P < 0.05$ vs. blank mice.

induction and the disruption of the redox state, providing an alternative pathway to boost the inflammatory response. Tan-IIA reduced succinate accumulation and prevented NLRP3 inflammasome activation, indicative of the potential for pharmaceutical intervention to be used in mitochondrial metabolism.

LPS stimulation significantly promoted macrophage polarization toward the M1 pro-inflammatory phenotype, which is predominately characterized by metabolic reprogramming from oxidative phosphorylation to glycolysis. In line with reported findings [11, 34], succinate was strongly upregulated in LPS-stimulated macrophages (Fig. 2b). The addition of succinate also significantly increased ROS production (Fig. 2d). It has been reported that glutamine-dependent anaplerosis is the principal supplier of succinate in LPS-stimulated macrophages [11]. Tan-IIA profoundly reversed this accumulation. Intriguingly, SDH was also induced; hence, the mitochondrial oxidation of succinate was greatly promoted in LPS-stimulated macrophages. Oxidation of succinate by SDH and mitochondrial hyperpolarization together drove ROS production to further promote IL-1β release. Although inhibition by DMM (an inhibitor of succinate oxidation) increased the levels of succinate [10], DMM still exhibited an anti-inflammatory outcome. The paradox between concurrent inhibition of succinate and SDH by Tan-IIA was probably associated with altered glycolysis and mitochondrial metabolism. These findings also indicated that there was an alternative pathway for succinate

generation, and Tan-IIA may largely decrease the supply of succinate by interrupting anaplerosis. Admittedly, further experiments are needed to determine the respective contributions of succinate and SDH inhibition to anti-inflammatory effects.

Similarly, the conspicuously overactivated SDH in mitochondria promoted mitochondrial ROS generation, which was probably pertinent to the raised mitochondrial membrane potential (Δψ$_m$). Δψ$_m$ is mainly generated in the process of proton pumping in mitochondrial membranes via complexes I, III, and IV [36]. The interruption of proton pumping via the complex I inhibitor rotenone significantly reduced mitochondrial ROS generation in our study (MitoSOX staining). However, hyperactivated SDH drove reverse electron transport (RET) through mitochondrial complex I. These findings suggested that ROS were generated at mitochondrial complex I owing to RET, since complex I is the major site for electron switching and leads to superoxide generation [37]. Additionally, the accumulated succinate was rapidly oxidized by SDH, leading to electrons moving back through complex I to generate ROS [13]. Tan-IIA suppressed succinate-driven mitochondrial ROS production. A previous study showed that Tan-IIA suppressed oxidative stress by upregulating Nrf2 in myofibroblasts [38]; herein, we showed that Tan-IIA reduced mitochondrial ROS production as a result of SDH oxidation inhibition.

In addition to mitochondrial metabolic dysfunction, cytosolic glycolysis was significantly strengthened after LPS stimulation. The

996

upregulated expression of HK-II and PKM2, as well as the increased lactate content, strongly indicated enhanced glycolysis. As the target genes of HIF-1α, both HK-II and PKM2 are pivotal rate-limiting elements responsible for glycolysis. The HIF-1α inhibitor PX-478 prevented the gene expression of HK-II and PKM2, further suggesting the involvement of HIF-1α in glycolysis regulation. Similar results were observed following Tan-IIA treatment. As a pivotal transcription regulator, the translocation of HIF-1α to the nucleus certainly promoted the expression of HIF-1α-dependent genes, including genes related to glycolysis and genes encoding pro-inflammatory proteins. HIF-1α is continuously degraded by PHD [39, 40]. The accumulated cytosolic succinate is reported to directly and indirectly (through ROS) suppress PHD in macrophages stimulated by LPS, which further stabilizes HIF-1α [11, 40]. Indeed, the addition of DS promoted the translocation of HIF-1α, while the succinate transporter inhibitor DEBM profoundly decreased HIF-1α expression. In this context, reducing succinate accumulation in the cytoplasm by Tan-IIA should directly contribute to the prevention of HIF-1α induction or stabilization. Interestingly, DMM or Tan-IIA alleviated the nuclear transition of HIF-1α, even though the BMDMs were challenged by DS. This result indicated that reducing succinate and interrupting succinate oxidation jointly produced the benefit of reducing HIF-1α signaling. Moreover, Tan-IIA also lowered HIF-1α expression by reducing mitochondrial ROS production, mimicking the effect of ROS scavengers.

HIF-1α activation transcriptionally upregulates genes involved in glycolysis, and the altered redox status is thought to be the cause of the reduced ratio of $NAD^+/NADH$. As a member of NAD^+-dependent deacetylases, the expression and activity of Sirt2 are tightly modulated in response to energy and redox status; because it is a fuel-sensing molecule, its expression and activity are adaptable [19]. As reported, Sirt2 expression is closely associated with the binding status of promotor regulatory elements [41, 42]. Its function is tightly regulated by posttranslational modifications and NAD^+ levels [43]. LPS stimulation resulted in decreased NAD^+ due to intracellular metabolic reprogramming, which further reduced the activity of Sirt2. Moreover, the mRNA and protein levels of Sirt2 were both downregulated after LPS stimulation. Tan-IIA upregulated the protein level of Sirt2 in a dose-dependent manner. Immunoprecipitation analysis clearly showed that a decrease in Sirt2 but not Sirt1 led to an increase in acetylation of α-tubulin in the cytosol. Tan-IIA increased the binding of Sirt2 to α-tubulin, explaining the reduced acetylation of Sirt2. Therefore, Tan-IIA restored the activity of Sirt2 by influencing its gene expression (Fig. 4a) as well as by affecting $NAD^+/NADH$ levels (Fig. 3f).

Because acetylated α-tubulin is a major component of microtubules responsible for the subcellular localization of NLRP3 and ASC, we reasoned that Tan-IIA-mediated decrease in α-tubulin acetylation should contribute to preventing NLRP3 inflammasome activation. Once activated, NLRP3 and its adapter ASC are both translocated to the perinuclear space, colocalizing with the endoplasmic reticulum and mitochondria [44]. Together, NLRP3 and ASC recruit pro-caspase-1 and then promote the activation of mature caspase-1, which is responsible for the process of IL-1β maturation. In this context, the successfully assembled inflammasome is responsible for the secretion of IL-1β into the extracellular matrix. Glycolysis resulting from metabolic reprogramming notably promotes the activation of the NLRP3 inflammasome via its major intermediates, such as succinate and NAD^+ [45]. Our results showed that Tan-IIA inactivated HIF-1α by SDH suppression, which restored Sirt2 activity by improving intracellular redox homeostasis. These actions may be involved in the suppression of NLRP3 inflammatory activation by Tan-IIA. Tan-IIA impaired the assembly of NLRP3 and ASC by suppressing the acetylation levels of α-tubulin, and the Sirt2 inhibitor AGK-2 diminished the inhibitory effects of Tan-IIA, providing evidence to validate our

speculation. Moreover, the anti-inflammatory action was further confirmed in LPS-challenged mice. Tan-IIA evidently restored the Sirt2 protein levels and downregulated NLRP3 protein in mice.

In summary, Tan-IIA remarkably inhibited mitochondrial ROS generation by interrupting SDH hyperactivation to further reduce HIF-1α stabilization and transcription. In addition, attenuation of glycolysis and preservation of Sirt2 activity contributed to the suppression of NLRP3 inflammatory activation. Although published studies have demonstrated that Tan-IIA suppresses the inflammatory response through different mechanisms [26, 27, 46], our findings provide new insight into the anti-inflammatory action of Tan-IIA with respect to metabolic and redox regulation.

AUTHOR CONTRIBUTIONS
QYL and YZ participated in the most of experimental performance, data analysis, and the preparation of the paper. QYL, YZ, XRS, QN, and QSS performed the animal experiments, primary BMDMs isolation and culture, the qPCR, Western blot analysis, immunoprecipitation and immunohistochemical analysis, etc. XNL and BLL were mainly involved in the improvement of paper. NL provided the technical support in sample preparation and data analysis. BLL, FH, and ZXQ designed and supervised the study, and revised the paper. All the authors approved the final version of the paper.

REFERENCES
1. Murray Peter J, Allen Judith E, Biswas Subhra K, Fisher Edward A, Gilroy Derek W, Goerdt S, et al. Macrophage activation and polarization: nomenclature and experimental guidelines. Immunity. 2014;41:14–20.
2. Kumar, V. Macrophages: The potent immunoregulatory innate immune cells. In: Bhat, KH (ed.). In macrophage activation-biology and disease. London, UK: IntechOpen, 2020.
3. El Kasmi KC, Stenmark KR. Contribution of metabolic reprogramming to macrophage plasticity and function. Semin Immunol. 2015;27:267–75.
4. Kelly B, O'Neill LA. Metabolic reprogramming in macrophages and dendritic cells in innate immunity. Cell Res. 2015;25:771–84.
5. Murray PJ. Macrophage polarization. Annu Rev Physiol. 2017;79:541–66.
6. Langston PK, Shibata M, Horng T. Metabolism supports macrophage activation. Front Immunol. 2017;8:61. https://doi.org/10.3389/fimmu.2017.00061.
7. O'Neill Luke AJ. A broken Krebs cycle in macrophages. Immunity. 2015;42:393–4.
8. Mills E, O'Neill LAJ. Succinate: a metabolic signal in inflammation. Trends Cell Biol. 2014;24:313–20.
9. Zorov DB, Juhaszova M, Sollott SJ. Mitochondrial reactive oxygen species (ROS) and ROS-induced ROS release. Physiol Rev. 2014;94:909–50.
10. Mills EL, Kelly B, Logan A, Costa ASH, Varma M, Bryant CE, et al. Succinate dehydrogenase supports metabolic repurposing of mitochondria to drive inflammatory macrophages. Cell. 2016;167:457–70.e13.
11. Tannahill GM, Curtis AM, Adamik J, Palsson-McDermott EM, McGettrick AF, Goel G, et al. Succinate is an inflammatory signal that induces IL-1beta through HIF-1alpha. Nature. 2013;496:238–42.
12. Corcoran SE, O'Neill LAJ. HIF1α and metabolic reprogramming in inflammation. J Clin Investig. 2016;126:3699–707.
13. Ryan DG, Murphy MP, Frezza C, Prag HA, Chouchani ET, O'Neill LA, et al. Coupling Krebs cycle metabolites to signalling in immunity and cancer. Nat Metab. 2019;1:16–33.
14. Brüne B, Dehne N, Grossmann N, Jung M, Namgaladze D, Schmid T, et al. Redox control of inflammation in macrophages. Antioxid Redox Sign. 2013;19:595–637.
15. Verdin E. NAD+ in aging, metabolism, and neurodegeneration. Science. 2015;350:1208–13.

Tan-IIA alleviates inflammation via inactivation of SDH
QY Liu et al.

997

16. Chalkiadaki A, Guarente L. Sirtuins mediate mammalian metabolic responses to nutrient availability. Nat Rev Endocrinol. 2012;8:287–96.

17. Verdin E, Hirschey MD, Finley LWS, Haigis MC. Sirtuin regulation of mitochondria: energy production, apoptosis, and signaling. Trends Biochem Sci. 2010; 35:669–75.

18. Webster BR, Lu Z, Sack MN, Scott I. The role of sirtuins in modulating redox stressors. Free Radic Biol Med. 2012;52:281–90.

19. Gomes P, Fleming Outeiro T, Cavadas C. Emerging role of Sirtuin 2 in the regulation of mammalian metabolism. Trends Pharmacol Sci. 2015;36:756–68.

20. Singh CK, Chhabra G, Ndiaye MA, Garcia-Peterson LM, Mack NJ, Ahmad N. The role of sirtuins in antioxidant and redox signaling. Antioxid Redox Signal. 2018;28:643–61.

21. Misawa T, Takahama M, Kozaki T, Lee H, Zou J, Saitoh T, et al. Microtubule-driven spatial arrangement of mitochondria promotes activation of the NLRP3 inflammasome. Nat Immunol. 2013;14:454–60.

22. Zhou R, Yazdi AS, Menu P, Tschopp J. A role for mitochondria in NLRP3 inflammasome activation. Nature. 2011;469:221–5.

23. Shang Q, Xu H, Huang L. Tanshinone IIA: a promising natural cardioprotective agent. Evid Based Complement Alternat Med. 2012;2012:716459. https://doi.org/10.1155/2012/716459.

24. Gao S, Liu Z, Li H, Little PJ, Liu P, Xu S. Cardiovascular actions and therapeutic potential of tanshinone IIA. Atherosclerosis. 2012;220:3–10.

25. Xu W, Yang J, Wu LM. Cardioprotective effects of tanshinone IIA on myocardial ischemia injury in rats. Pharmazie. 2009;64:332–6.

26. Fan G, Jiang X, Wu X, Fordjour PA, Miao L, Zhang H, et al. Anti-inflammatory activity of tanshinone IIA in LPS-stimulated RAW264.7 macrophages via miRNAs and TLR4-NF-kappaB pathway. Inflammation. 2016;39:375–84.

27. Fan GW, Gao XM, Wang H, Zhu Y, Zhang J, Hu LM, et al. The anti-inflammatory activities of tanshinone IIA, an active component of TCM, are mediated by estrogen receptor activation and inhibition of iNOS. J Steroid Biochem. 2009;113:275–80.

28. Feng J, Li S, Chen H. Tanshinone IIA inhibits myocardial remodeling induced by pressure overload via suppressing oxidative stress and inflammation: possible role of silent information regulator 1. Eur J Pharmacol. 2016; 791:632–9.

29. Shu M, Hu XR, Hung ZA, Huang DD, Zhang S. Effects of tanshinone IIA on fibrosis in a rat model of cirrhosis through heme oxygenase-1, inflammation, oxidative stress and apoptosis. Mol Med Rep. 2016;13:3036–42.

30. Baolin L, Inami Y, Tanaka H, Inagaki N, Iinuma M, Nagai H. Resveratrol inhibits the release of mediators from bone marrow-derived mouse mast cells in vitro. Planta Med. 2004;70:305–9.

31. Mantovani A, Sica A, Locati M. Macrophage polarization comes of age. Immunity. 2005;23:344–6.

32. Zhao YP, Wang F, Jiang W, Liu J, Liu BL, Qi LW, et al. A mitochondrion-targeting tanshinone IIA derivative attenuates myocardial hypoxia reoxygenation injury through a SDH-dependent antioxidant mechanism. J Drug Target. 2019;27:896–902.

33. Muendlein HI, Poltorak A. Flipping the switch from inflammation to cell death. Trends Immunol. 2020;41:648–51.

34. Tretter L, Patocs A, Chinopoulos C. Succinate, an intermediate in metabolism, signal transduction, ROS, hypoxia, and tumorigenesis. Biochim Biophys Acta. 2016;1857:1086–101.

35. Mills EL, O'Neill LA. Reprogramming mitochondrial metabolism in macrophages as an anti-inflammatory signal. Eur J Immunol. 2016;46:13–21.

36. Sanin DE, Matsushita M, Klein Geltink RI, Grzes KM, van Teijlingen Bakker N, Corrado M, et al. Mitochondrial membrane potential regulates nuclear gene expression in macrophages exposed to prostaglandin E2. Immunity. 2018;49:1021–33.e6.

37. Hirst J, King M, Pryde K. The production of reactive oxygen species by complex I. Biochem Soc Trans. 2008;36:976–80.

38. An L, Peng LY, Sun NY, Yang YL, Zhang XW, Li B, et al. Tanshinone IIA activates nuclear factor-erythroid 2-related factor 2 to restrain pulmonary fibrosis via regulation of redox homeostasis and glutaminolysis. Antioxid Redox Sign. 2019;30:1831–48.

39. Sharma M, Boytard L, Hadi T, Koelwyn G, Simon R, Ouimet M, et al. Enhanced glycolysis and HIF-1α activation in adipose tissue macrophages sustains local and systemic interleukin-1β production in obesity. Sci Rep. 2020;10:5555.

40. Selak MA, Armour SM, MacKenzie ED, Boulahbel H, Watson DG, Mansfield KD, et al. Succinate links TCA cycle dysfunction to oncogenesis by inhibiting HIF-α prolyl hydroxylase. Cancer Cell. 2005;7:77–85.

41. Liu T, Yang W, Pang S, Yu S, Yan B. Functional genetic variants within the SIRT2 gene promoter in type 2 diabetes mellitus. Diabetes Res Clin Pract. 2018;137:200–7.

42. Anwar T, Khosla S, Ramakrishna G. Increased expression of SIRT2 is a novel marker of cellular senescence and is dependent on wild type p53 status. Cell Cycle. 2016;15:1883–97.

43. Flick F, Lüscher B. Regulation of sirtuin function by posttranslational modifications. Front Pharmacol. 2012;3:29. https://doi.org/10.3389/fphar.2012.00029.

44. Sutterwala FS, Haasken S, Cassel SL. Mechanism of NLRP3 inflammasome activation. Ann N Y Acad Sci. 2014;1319:82–95.

45. Jiang D, Chen S, Sun R, Zhang X, Wang D. The NLRP3 inflammasome: role in metabolic disorders and regulation by metabolic pathways. Cancer Lett. 2018;419:8–19.

46. Zhang WL, Cao YA, Xia J, Tian L, Yang L, Peng CS. Neuroprotective effect of tanshinone IIA weakens spastic cerebral palsy through inflammation, p38MAPK and VEGF in neonatal rats. Mol Med Rep. 2018;17:2012–8.